**49th AIAA/ASME/ASCE/AHS/ASC Structures, Structural Dynamics, and Materials Conference
 16t**
7 - 10 April 2008, Schaumburg, IL

AIAA 2008-1820

Prediction of Bifurcation Onset of Large Order Aeroelastic Models

K.J. Badcock [*] and M.A.Woodgate [†]

Computational Fluid Dynamics Laboratory,

Flight Sciences and Technology,

Department of Engineering,

University of Liverpool,

L69 3BX, United Kingdom.

Computational aeroelasticity has become an active area of research in the past decade. Effort has been put into coupling between Computational Fluid Dynamic and Finite Element solvers, and model reduction to make the resulting simulations more useful for practical analysis. This paper is the latest in a series which describe research towards making eigenvalue based stability analysis routine for large scale CFD based semi-discrete systems. The particular contribution of this paper is to formulate the problem in a framework which exploits the Schur complement. This effectively allows the different parts of the system Jacobian to be treated in a decoupled way, with the final result being a small nonlinear eigenvalue problem for the stability analysis. The calculation of this small system can be done robustly in parallel. Results to illustrate the performance of the method are presented for model wings and full aircraft test cases.

I.   NOMENCLATURE

Symbols

A	Jacobian matrix
p	eigenvector
R	Residual vector of the fluid and/or structural model
S	Schur complement matrix
w	vector of fluid and/or structural unknowns

Greek

λ	eigenvalue
μ	Bifurcation parameter (altitude)

Subscripts

f	fluid model
s	structural model
0	equilibrium

---

[*]Professor, corresponding author. Tel. : +44(0)151 794 4847 , Fax. : +44(0)151 794 6841, Email : K.J.Badcock@liverpool.ac.uk

[†]Research Assistant

American Institute of Aeronautics and Astronautics

II.   Introduction

The system derived from coupling a Computational Fluid Dynamicis (CFD) code with a Finite Element Method (FEM) can be used in different ways to simulate the aeroelastic behaviour of an aircraft. The advancement of the coupled system in time can give information about the response to an initial disturbance, and hence the system stability.[1] This approach however must carry the cost of the unsteady CFD simulation and is unattractive for this reason, particularly when a large parameter space must be investigated. An additional drawback is that the time domain approach does not fit with the conventional approach to aircraft aeroelasticity, which is to examine the influence of the aerodynamics on the structural normal modes, and to look at the interaction of the aeroelastic modes.

An alternative is to use the coupled system to generate response information to forced inputs. The information is then used to setup a data driven model.[2] The data driven model is used to investigate the system free response at much lower cost than the full order system. However the data driven models are only applicable within the support of the data used to generate them. They are often formulated to be linearisations about a mean state, which will more than likely depend on the system parameters as well. If this is taken into account then the calculations required to generate the model can be quite extensive, driving up the total cost of the method.

An alternative is to stick with the full order system but to exploit some property of the dynamics to reduce the computational cost. One example is the Harmonic Balance method which assumes that the unstable response of the system is at a set of discrete frequencies (typically one).[3] The assumed harmonic content is used to reduce the cost of calculations to the equivalent of a few steady state calculations for an assumed response frequency, although a clear evaluation on computational cost is not available in the literature.

The approach used in the current paper is to view the problem of computing flutter onset as a stability problem for a steady state of the coupled system. Assuming a Hopf Bifurcation, stability is lost when the system Jacobian matrix has a pair of eigenvalues which cross the imaginary axis. The idea is to compute when this happens at a computational cost much less than time domain analysis.

This was first attempted for a symmetric aerofoil free to move in pitch and plunge.[4] The coupled system of equations was augmented by an equation for a purely imaginary eigenvalue. The augmented system was solved using Newton's method. Approximations were made to make the direct solution of the linear system for the updates more tractable. Unfortunately these approximations degraded the convergence and robustness of the method.

These problems were overcome by using an iterative linear solver.[5] The method was extended to three dimensional cases in.[6] A problem with the augmented system is that the Newton iterations require the second Jacobian in the coefficient matrix. It is unfeasible to form this matrix explicitly. For symmetric problems the calculation of the steady state is independent of the dynamic pressure and the equilibrium can be calculated separately from the behaviour of the eigensystem.[4–6] In this case the second Jacobian is not needed. However, in the general case the steady state and the eigensystem must be calculated in a coupled manner.

To overcome this problem, the classical shifted inverse power method (IPM) was adapted to track eigenvalues as the dynamic pressure changes.[7] This method solves a system very similar to the augmented system, but the steady state can be updated for each value of the dynamic pressure before the eigenvalue is calculated. The output of the method is a locus of the aeroelastic system eigenvalues. In a manner identical to classical linear flutter analysis, the frequency and damping values can be tracked, and the value of dynamic pressure where the damping is lost for any mode located.

There were two limitations with the method as presented. First, a parallel implementation was needed to deal with realistically sized models. Secondly, the mode tracking was not sufficiently robust. The central computational problem involved with calculating stability through eigenvalues is that the linear system (at least in the approaches based on tracking individual eigenvalues through shift and invert methods) invariably ends up being increasingly ill-conditioned as the eigenvalue is approached. The linear system is then very difficult to solve , particularly when extra approximations are needed to obtain a preconditioner which can be calculated in parallel.

The current paper aims to avoid the problem of solving linear systems with a coefficient matrix which is almost singular through a reformulation using the Schur complement. The reformulation leads to a small nonlinear eigenvalue problem which can be solved over an

American Institute of Aeronautics and Astronautics

altitude range at very low computational cost. In the process the mode tracking problem is solved since very small increments of altitude can be used. This paper continues with a brief summary of the underlying coupled CFD-FEM system. The Schur complement eigenvalue formulation is then described. Results are given for 4 test problems to illustrate the performance of the method. The paper finishes with conclusions.

III.   Coupled Formulation

The semi-discrete form of the coupled CFD-FEM system is written as

$$\frac{d\mathbf{w}}{dt} = \mathbf{R}(\mathbf{w}, \mu) \tag{1}$$

where

$$\mathbf{w} = [\mathbf{w}_f, \mathbf{w}_s]^T \tag{2}$$

is a vector containing the fluid unknowns ($\mathbf{w}_f$) and the structural unknowns ($\mathbf{w}_s$), and

$$\mathbf{R} = [\mathbf{R}_f, \mathbf{R}_s]^T \tag{3}$$

is a vector containing the fluid residual ($\mathbf{R}_f$) and the structural residual ($\mathbf{R}_s$). The residual also depends on a parameter μ (in this paper μ is altitude) which is independent of $\mathbf{w}$. An equilibrium $\mathbf{w}_0(\mu)$ of this system satisfies $\mathbf{R}(\mathbf{w}_0, \mu) = \mathbf{0}$.

The stability of equilibria of equation 1 is determined by eigenvalues of the Jacobian matrix $A = \partial \mathbf{R} / \partial \mathbf{w}$. In the examples considered in the current paper, stability is lost through a Hopf Bifurcation where a complex conjugate pair of eigenvalues of A crosses the imaginary axis.

The calculation of the Jacobian A is most conveniently done by partitioning the matrix as

$$A = \left[\begin{array}{cc} \frac{\partial \mathbf{R}_f}{\partial \mathbf{w}_f} & \frac{\partial \mathbf{R}_f}{\partial \mathbf{w}_s} \\ \frac{\partial \mathbf{R}_s}{\partial \mathbf{w}_f} & \frac{\partial \mathbf{R}_s}{\partial \mathbf{w}_s} \end{array} \right] = \left[\begin{array}{cc} A_{ff} & A_{fs} \\ A_{sf} & A_{ss} \end{array} \right]. \tag{4}$$

The block A_{ff} is a large sparse matrix derived by differentiating the CFD residual (built up from fluxes calculated using Osher's method, which is differentiable everywhere) with respect to the CFD cell values. This is a non-trivial task, but has nonetheless been done analytically. The term A_{fs} arises from the dependence of the CFD residual on the mesh motion and speeds, which in turn depend on the structural solution. These terms are currently evaluated using finite differences. The term A_{sf} is due to the dependence of the generalised forces on the surface pressures. Finally, A_{ss} is the Jacobian of the structural equations with respect to the structural unknowns. The details of the Jacobian calculation are given in references[5] and.[6]

In the current work, and as is conventional in aircraft aeroelasticity, the structure is modelled by a small number of modes, and so the number of the fluid unknowns is far higher than the structural unknowns. This means that the Jacobian matrix has a large, but sparse, block A_{ff} surrounded by thin strips for A_{fs} and A_{sf}.

IV.   Schur Complement Eigenvalue Solver

The stability calculation is formulated as an eigenvalue problem. The task is to find the eigenvalues of the matrix in equation 4 which have the most positive real part. To focus this search, the aeroelastic eigenvalue problem can be viewed as tracking the structural normal modes when they are under the influence of the fluid. This follows the well established approach for linear analysis. The structural eigenvalues are those of the block A_{ss}, which has the dimension $2n$ where n is the number of normal modes retained from the structural model.

Now, write the coupled system eigenvalue problem as

$$\left[\begin{array}{cc} A_{ff} & A_{fs} \\ A_{sf} & A_{ss} \end{array} \right] \mathbf{p} = \lambda \mathbf{p} \tag{5}$$

where $\mathbf{p}$ and λ are the complex eigenvector and eigenvalue respectively. Partition the eigenvector as

$$\mathbf{p} = [\mathbf{p}_f, \mathbf{p}_s].^T \tag{6}$$

American Institute of Aeronautics and Astronautics

It can be shown[8] that the eigenvalue λ (assuming it is not an eigenvalue of A_{ff}) satisfies the nonlinear eigenvalue problem

$$S(\lambda)\mathbf{p}_s = \lambda\mathbf{p}_s \tag{7}$$

where $S(\lambda) = A_{ss} - A_{sf}(A_{ff} - \lambda I)^{-1}A_{fs}$. Looking to this nonlinear eigenvalue problem, the matrix $S(\lambda)$ has the following features. First, it is the sum of the structural matrix and a second term (refered to here as the correction matrix) which arises from the coupling with the fluid model. As the coupling is reduced to zero, through increasing the altitude, the structural matrix is recovered and an eigenvalue of the uncoupled system is then obtained. Secondly, the correction matrix depends on the eigenvalue, producing a *frequency matching* with the aerodynamics as part of the solution method. Thirdly, the inverse of the matrix $A_{ff} - \lambda I$ is required, and importantly, λ is not an eigenvalue of A_{ff}, avoiding the ill-conditioning which would arise if this was not the case.

The nonlinear equation **7** is solved using Newton's method. Each iteration requires the formation of the residual and its Jacobian matrix. The formation of the correction matrix is required to form the Jacobian matrix. This can be achieved through $2n$ solutions of a linear system against $A_{ff} - \lambda I$, one for each column of A_{fs}. These solutions are then multiplied against A_{sf}. Now, for each value of the bifurcation parameter, there are n solutions of the nonlinear system in equation **7**, and so the cost of forming the correction matrix at each Newton step, for each solution and for a range of parameters becomes too high. To overcome this the expansion

$$(A_{ff} - \lambda I)^{-1} = A_{ff}^{-1} + \lambda A_{ff}^{-1}A_{ff}^{-1} + \lambda^2 A_{ff}^{-1}A_{ff}^{-1}A_{ff}^{-1} + ... \tag{8}$$

is used where λ must be small for the series to converge. Note that this restriction can be overcome by assuming that the eigenvalue we are calculating is a small change from the eigenvalue λ_0 of A_{ss}. Then λ_0 can be used as a shift to the full system eigenvalue problem by replacing A_{ff} by $A_{ff} - \lambda_0 I$ and A_{ss} by $A_{ss} - \lambda_0$. This modifies the nonlinear eigenvalue problem in equation **7** by redefining $S(\lambda) = (A_{ss} - \lambda_0 I) - A_{sf}(A_{ff} - \lambda_0 I - \lambda I)^{-1}A_{fs}$. Now the series approximation becomes

$$(A_{ff} - \lambda_0 I - \lambda I)^{-1} = (A_{ff} - \lambda_0 I)^{-1} + \lambda(A_{ff} - \lambda_0 I)^{-2} + \lambda^2(A_{ff} - \lambda_0 I)^{-3} + ... \tag{9}$$

where λ is a small change to λ_0. When the nonlinear eigenvalue problem is solved for λ, the eigenvalue of the original system is then $\lambda_0 + \lambda$.

Note that the value of λ is decoupled from the matrix inverse through the use of the series expansion. Also if the altitude is the bifurcation parameter, then the dynamic pressure can be pulled out of the correction matrix as a coefficient. The nonlinear system can then be formulated in the following way:

1. Select the normal mode to be tracked - denote the eigenvalue shift as λ_0 which is the frequency of the normal mode

2. Truncating the series expansion at **2** terms, calculate $(A_{ff} - \lambda_0 I)^{-1}A_{fs}$, $(A_{ff} - \lambda_0 I)^{-2}A_{fs}$. This requires 4n linear systems to be solved where n is the number of normal modes retained.

3. Solve Newton's method using the correction matrix with the series expansion used to generate the left hand side Jacobian matrix for the Schur eigenvalue problem. The right hand side residual can be evaluated using the series expansion (referred to in this paper as the *series method* or by one linear system solve against the matrix $(A_{ff} - \lambda_0 I - \lambda I)$ (referred to as the *nonlinear method*). The consideration here is how large λ has become. If it is small then the series expansion can be used for the residual without incurring significant error. Results below will show that this behaviour can be anticipated.

Solutions of the nonlinear eigenvalue problem are traced out for values of the bifurcation parameter (the altitude in this paper). If the series method is used then very small increments of the parameter can be used, since once the correction matrix is generated, the cost of solving the nonlinear eigenvalue problems is almost negligible. On the other hand if the nonlinear method is used, then the series solutions can act as an initial guess for the nonlinear method, which is solved at larger parameter increments. If the Newton method fails to converge then this indicates that the series approximation has become too poor to drive convergence, and the correction matrix can be regenerated with the best approximation to the eigenvalue at the current altitude as the new shift. In the cases computed for this paper this was never necessary. The two options have both been found to give very robust mode tracking.

American Institute of Aeronautics and Astronautics

V.   Parallel Implementation of the Linear Solver

The sparse linear system to generate the correction matrix is solved using the Generalized Conjugate Residual (GCR) algorithm.[10] The crucial aspect of the solution is the preconditioning. Some options previously considered are discussed in reference.[9] In summary:

1. The Block Incomplete Upper Lower (BILU) factorisation, with one or two levels of fill-in, of the matrix $A_{ff}^* - \lambda_0 I$ is used.

2. Here, A^* is an average of the Jacobian matrix derived when using the first order spatial discretisation for the CFD residual and the matrix A_{ff} (based on the second order spatial scheme). Experiments have shown that the factorisation based on A_{ff} makes a poor preconditioner, possibly due to the factorisation being unstable.

3. The factorisation is done in terms of complex variables, which appears to improve the quality of the preconditioner.

4. The terms in the coefficient matrix of the linear system are included for the matrix-vector products, and so the converged solution of the CGR iterations will not be polluted by approximations made for the preconditioning.

5. For parallel calculations the factorisation is blocked on each processor. It is possible to improve on this by using some form of Schwartz or Schur preconditioning with inner iterations.[11]

Previous experience with solving a linear system against the shifted form of the coupled matrix given in equation 4 was that the preconditioning described above is inadequate as the number of processors increases. This is likely to be because the matrix becomes singular as the shift tends towards an eigenvalue. In the Schur formulation this problem is avoided, and in all of the applications computed for this paper the linear system was solved (defined as driving the initial residual down by **7** orders of magnitude) on average in about **100** steps, and never more than **220** steps.

VI.   Results

A.   Goland Wing

The Goland wing, shown in figure 1, has a chord of **6** feet and a span of **20** feet. It is a rectangular cantilevered wing with a 4% thick parabolic section. The structural model follows the description given in reference,[12] and is shown in figure 1. The CFD grid is block structured and uses an O-O topology. This allows points to be focussed in the tip region which is most critical for the aerodynamic contribution to the aeroelastic response. The fine grid has **236** thousand points and a coarse level was extracted from this grid, which has **35** thousand points. Views of the fine grid are shown in figure 1. Four mode shapes were retained for the aeroelastic simulation. The mapped modes on the CFD surface grid are shown in figure **2**.

The test case has a tip store in the structural model. This case is interesting because it leads to a bucket of shock induced limit cycle oscillation for a freestream Mach number of around **0.92**. This was investigated in reference,[7] which also included a review of previous studies and the prediction of the LCO amplitude using a model reduction based on the critical eigenvector. The Goland wing is very flexible and leads to instability within the flight envelope at all high subsonic freetsream Mach numbers. The case is particularly useful in the current work to test the validity of the series expansion when there are significant changes in the aeroelastic eigenvalue as the altitude is reduced.

The correction matrices were first calculated, for a number of Mach numbers in the range **0.3** to **0.97**, at the highest of the altitude range considered(-10 to 30 thousand feet). All calculations have a zero angle of attack. The matrices were calculated on the coarse and fine grids, with the fine grid calculations being done in parallel on 8 processors. The convergence of the linear solver during these calculations was good for all cases, with around **30** linear solver steps per column calculated required on the coarse grid and around **80** on the fine grid. The eigenvalues were then traced based on these matrices. Four different types of behaviour were observed, and are illustrated in figure 3. First, at low Mach numbers (such as Mach 0.3 in figure 3), no instability is predicted in the altitude range. This is in agreement (as expected) with linear predictions obtained by running NASTRAN.
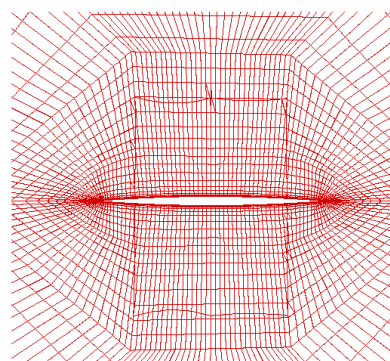
American Institute of Aeronautics and Astronautics
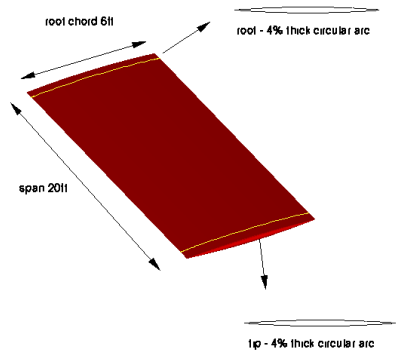
Summary of Geometry
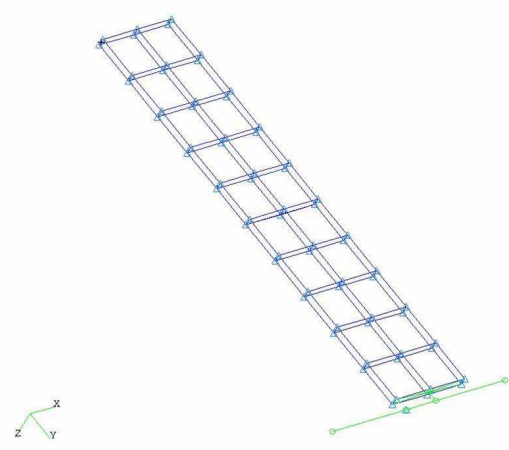
FE mesh
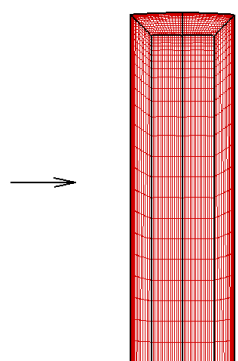
surface CFD grid

slice from volume CFD grid

Figure 1. Views of geometry, FE and CFD Grids for Goland Wing.

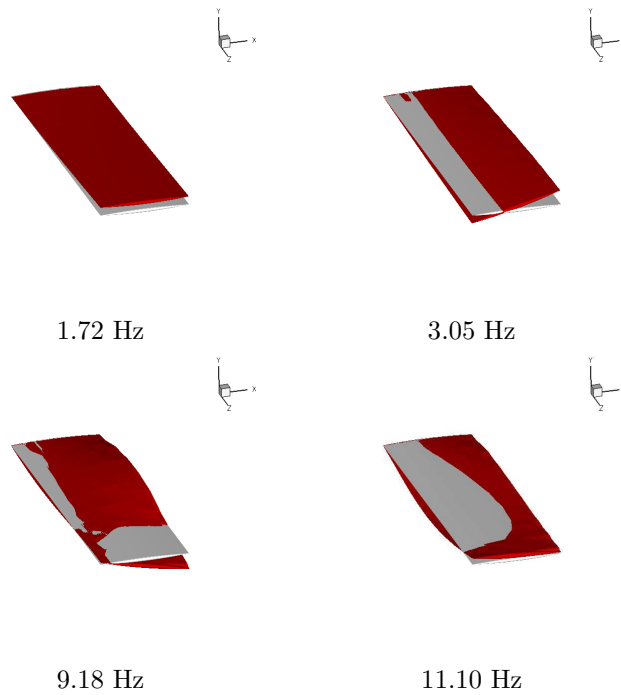American Institute of Aeronautics and Astronautics

Figure 2. Mode Shapes mapped to the CFD surface grid for Goland wing.

Secondly, as the Mach number is increased the first bending and torsion modes interact, with the real part of the bending mode eigenvalue becoming positive within the altitude range. An example of this behaviour at Mach 0.8 is shown in figure 3. The quantitative agreement with NASTRAN is also good for this behaviour as indicated on the plot of the real part. This is expected because the instability is not yet driven by shock waves. With increasing freestream Mach number a strong shock develops towards the trailing edge of the wing, as shown in figure 3 at Mach 0.92. Now the torsion mode is unstable at all points in the altitude range, as shown in the plot of variation of the real part of the eigenvalue. At this point NASTRAN also predicts that all modes are unstable, although this must be for reasons other than the presence of shock waves. Finally, at higher freestream Mach numbers the shock reaches the trailing edge and the wing recovers stability at higher altitude (Mach 0.97 in the figure). The flutter mechanism changes with an interaction observed between the second torsion and bending modes. NASTRAN continues to predict instability at all points in the altitude range.

The consistency of the results was evaluated in three ways. First, comparisons with NASTRAN showed agreement at low freestream Mach numbers as expected, since the aerodynamic predictions from the Euler equations and the potential theory should be similar in the absence of significant nonlinear compressible effects. Secondly, the eigenvalues traced for the fine (solid lines) and coarse (dashed lines) grids are both shown in figure 3 and are in good agreement. Finally, and most importantly, the influence of the series expansion on the accuracy of the predicted eigenvalues was considered. This was done by solving the Schur eigenvalue problem using an evaluation of $S(\lambda)$, by solving a linear system against $A_{ff} - \lambda I$, rather than using the series expansion given in equation 9 to simplify this computational task. The results from the former approach are plotted using points in figure 3, labelled as *nonlinear*. Even with significant changes in the eigenvalue real and imaginary parts over the altitude range, the predictions using the series expansion are shown to be excellent for this case.

For the fine grid and on 8 processors, the time required to calculate a steady state was 11 minutes, the time to form the correction matrix was 137 mins (with the eigenvalue curves over the whole altitude range then computed at virtually no extra cost after this), and the time to compute the four sets of eigenvalues using the nonlinear method at 8 values of altitude being an additional 202 minutes, with an average of 3 iterations per eigenvalue. The necessary wall clock time on 8 processors to compute one flutter point is therefore

American Institute of Aeronautics and Astronautics

13.5 times the cost of a steady state solution.

B. SST Control Surface Buzz

The second test case is based on the transonic aeroelastic experiments performed at the National Aerospace Laboratory of Japan.[13] One of the motivations for the experiments was to generate a set of results against which aeroelastic codes could be validated. For this reason, along with the unsteady pressure distribution over the wing, the dynamic deformation and unsteady force coefficients were also measured. The SST arrow wing is a cranked double delta with a root chord of 2.103 metres. A half model was used in the experiments with a semi-span of 1 metre. The section profile is a NACA 0003. The inboard delta has a sweep angle of $72.8°$ and outboard the sweep is $51.6°$. The trailing edge flap starts at 20% half-span and terminates at 50% half-span, with a flap chord of 0.11 metres. The geometry is summarised in figure 4.

Experimental pressure and deformation data was collected at transonic Mach numbers, low angles of attack and for forced flap motions at various amplitudes and frequencies. This data was used to investigate the use of a blended flap treatment.[14] Evaluation was made for the structural response and the unsteady aerodynamics resulting from forced flap motions. This work was extended in the thesis of Rampurawala[15] to investigate shock induced buzz using time domain analysis. In the current paper the eigenvalues of the system are used to compute the onset Mach number for buzz.

For the CFD grid, a C-Type grid topology is used over the wing leading edge, the wing tip and also around the fuselage. The blocks at the trailing edge are of H-Type. Points are clustered around the trailing edge and the flap region where a shock is likely to develop and move. The grid has 234 thousand points, with the gap between the flap edges and the wing blended over.[14]

The structure of the SST was modelled as a 2D plate. The flap is modelled as a separate rigid plate attached to the main wing through springs. The spring stiffness constant was adjusted to give a flap frequency of 16.2 Hz which is within the realistic frequency range of a mechanically constrained trailing edge control surface. A plot of the control surface deflection is shown in figure 5. This is defined on the CFD surface grid, and indicates the blending treatment used. The flap mode was the only one retained for the current calculations.

Previously computed time domain responses for the control surface[15] showed that in the freestream Mach number range 0.9-0.98 a shock moves onto the control surface and a limit cycle oscillation is established. The precise onset Mach number depends on the magnitude of the initial disturbance, and whether this is enough to move a shock from ahead of the hinge line over the control surface. The analysis used in the current paper is unable to predict this effect, as it is a linear stability analysis about a nonlinear steady state. All calculations in the current paper were run at zero angle of attack.

The altitude range used was -5000 to 20000 metres. The eigenvalue associated with the flap mode was traced through this altitude for Mach numbers of 0.9 and then 0.95-1.0 in steps of 0.01. The resulting plots of the real and imaginary parts is shown in figure 6. There are two distinct cases observed. First, for Mach numbers below 0.98, the mode is damped at all values of altitude. In contrast, at Mach 0.99 and 1.00, the mode is undamped at all values of altitude. The reason for this is clear from the plots of surface pressure coefficient shown in figure 7. Here the location of the shock is clearly visible, with the shock moving onto the control surface at Mach 0.99. The outline of the control surface is indicated in black on these plots.

Again the predictions using the series (lines) and nonlinear (dots) methods were compared and are in excellent agreement (see figure 6). These calculations were run on 8 processors and the cost of calculating the steady state was 14 minutes, and of generating the correction matrix was 9 minutes. The nonlinear solution at 8 values of altitude required 49 minutes for 23 nonlinear steps (roughly 3 per eigenvalue). Hence for this case, to compute the critical Mach number required an equivalent computational cost of 11.5 steady solves (i.e. 7 Mach numbers times a cost of 1.64 steady solves at each Mach number).

C. Transport Wing

The MDO wing is a commercial transport wing, with a span of 36 metres, designed to fly in the transonic regime[16].[17] The profile is a thick supercritical section. The geometry is
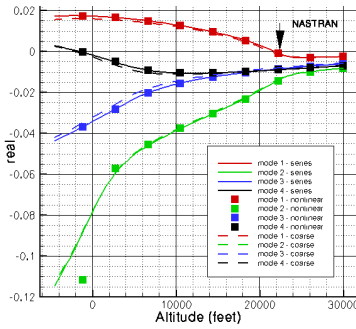
American Institute of Aeronautics and Astronautics
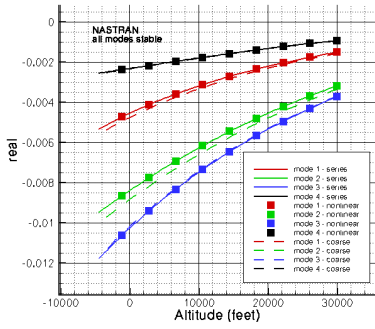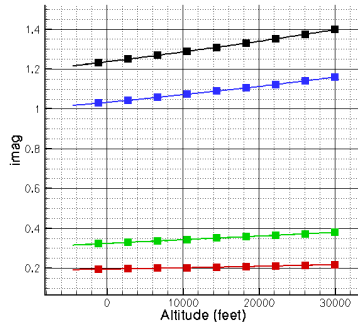
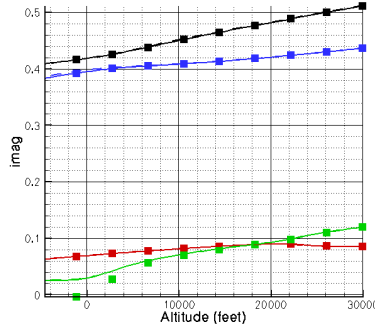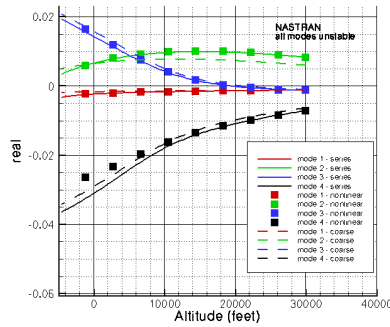Mach 0.3 real   Mach 0.3 imaginary   Mach 0.3 surface cp
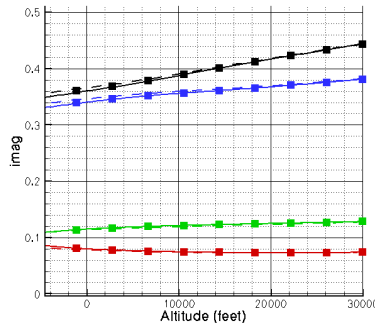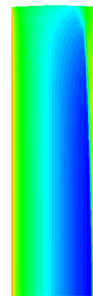
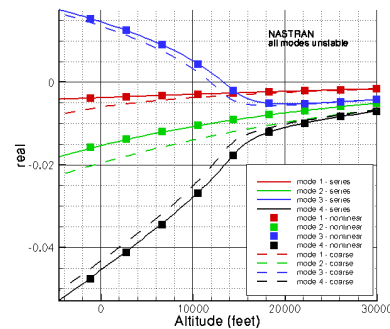Mach 0.8 real   Mach 0.8 imaginary   Mach 0.8 surface cp
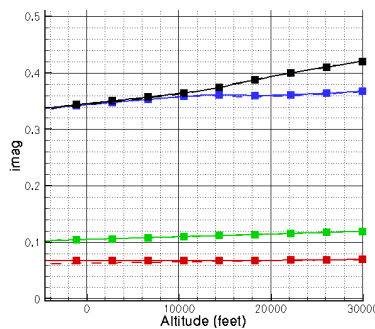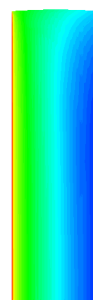
Mach 0.92 real   Mach 0.92 imaginary   Mach 0.92 surface cp
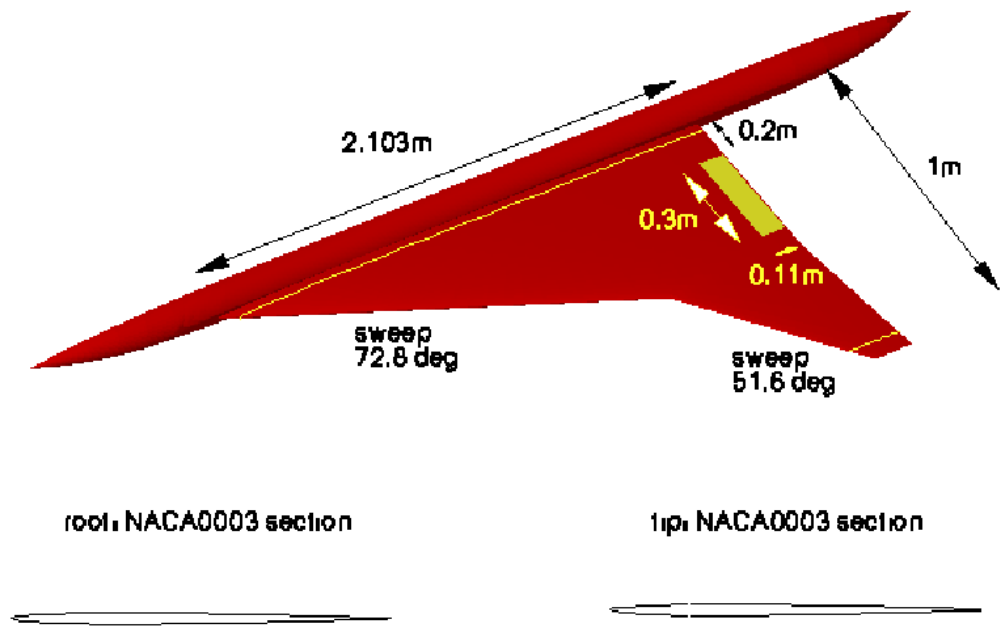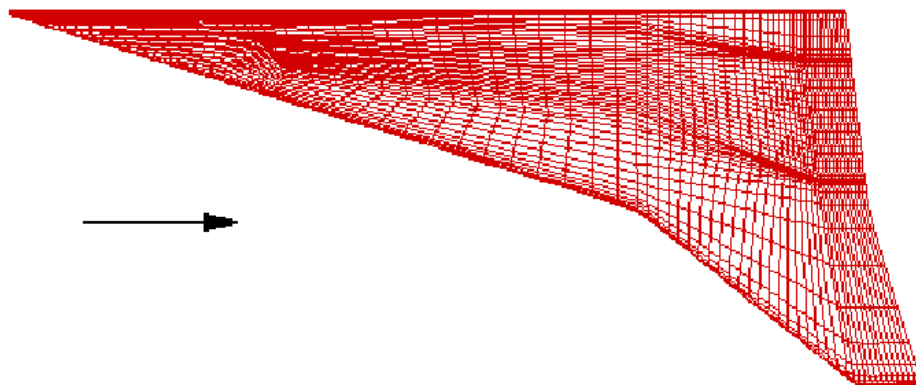
Mach 0.97 real   Mach 0.97 imaginary   Mach 0.92 surface cp

Figure 3. Variation of Real and Imaginary parts with altitude for Goland wing, together with surface pressure distributions showing the shock wave development.
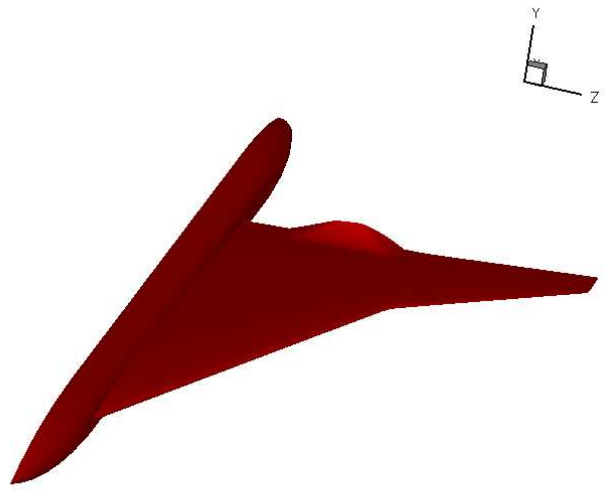
American Institute of Aeronautics and Astronautics

2.103m   0.2m

0.3m   1m

0.11m

sweep
72.8 deg

sweep
51.6 deg

root: NACA0003 section   tip: NACA0003 section

Summary of Geometry

Surface Grid

Figure 4. SST geometry and surface grid.

American Institute of Aeronautics and Astronautics

16.20 Hz

Figure 5. Deflected control surface defined on the CFD surface grid for the SST configuration.

real

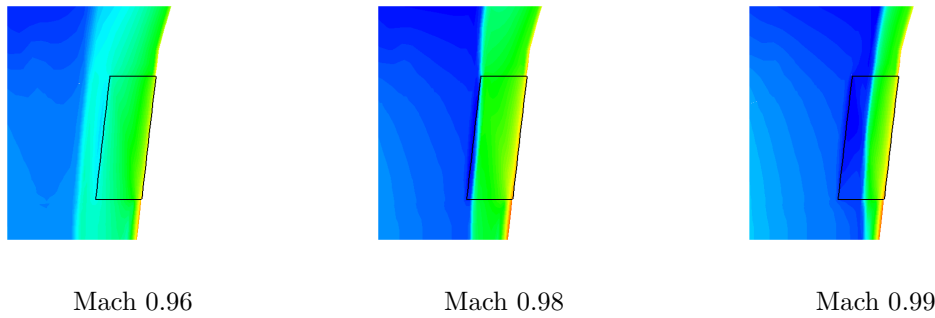imaginary
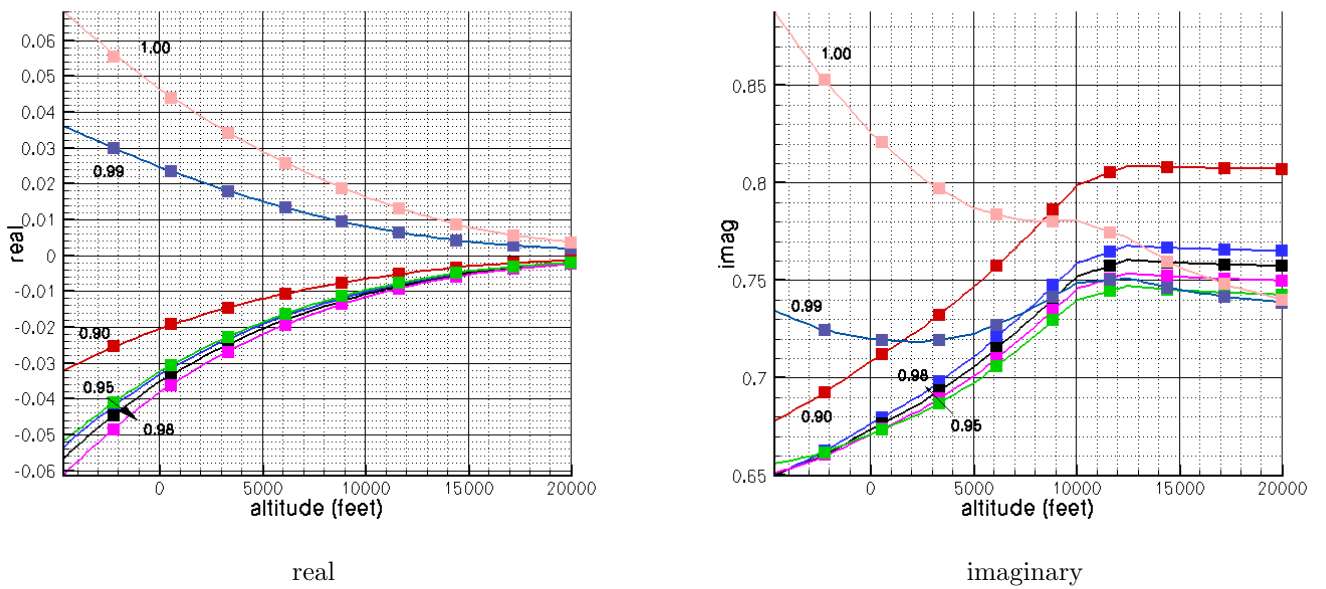
Figure 6. SST configuration.

American Institute of Aeronautics and Astronautics

Mach 0.96	Mach 0.98	Mach 0.99

Figure 7. Surface pressure coefficient distributions for different freestream Mach numbers for SST configuration.

summarised in figure 8. The structure is modelled as a wing box running down the central portion of the wing. The problems of mapping this reduced planform to the full planform CFD model are considered in reference.[18] The CFD grid used has 81 thousand points and is shown in figure 8. Results generated using the inverse power method to track eigenvalues were previously shown.[7] In the current work 8 modes are retained and the mapped modes on the fluid surface grid are shown in figure 9.

The feature of this test case is the larger number of modes. The altitude range was chosen to be 0 to 20000 metres. The first wing bending and torsion modes interact to give flutter at just below 5000 metres at Mach 0.85 and zero degrees angle of attack. Again the series and nonlinear predictions are compared and this time show some discrepancy as the bending mode loses damping. However, for all modes there is good qualitative and quantitative agreement. These results suggest that a good strategy would be to compute the eigenvalues using the series method, and then to check only the mode that is critical using the nonlinear approach. Note that no aerostatic deflection was included for these results. The development of a shock wave, particularly strong at the tip, is shown in figure 11. The shock is significantly weakened by a nose down aerostatic deflection at the tip.

The steady calculation took 22 minutes on 8 processors, and the correction matrix was generated in a total of 95 minutes for the eight modes. The time for the steady state solution is high for this case because smaller CFL numbers were required. The nonlinear solution required an average of 3 steps per eigenvalue, for a total of 72 minutes using 8 values of altitude for each mode. Hence in this case the flutter points required around 5 times the cost of a steady state solution.

D.   Generic Fighter Model

Finally, the Schur method is exercised on a model approximating a full aircraft. The intention here is to show that the method can scale to models of the size required for the analysis of real aircraft. The generic fighter was built on data publically available for the F-16 aircraft, since this has been the subject of much interest from an aeroelastic viewpoint. The approach was to establish a test case which is recognisable as an aircraft, and it obviously cannot be representative of the actual behaviour of the F-16.

The geometry is summarised in figure 12. A fuselage, wing and tip launcher were included as the minimum components required. The wing has a NACA64A204 section, and is twisted nose down 2.3 degrees from the root to the tip. The aircraft dimensions have been roughly based on the F-16.

A block structured grid was generated which has 890 thousand points and 240 blocks for the full configuration. The full span grid was obtained by reflecting a half span grid. The surface grid is shown in figure 12 and shows that the points are concentrated on the wing which contributes most to the aeroelastic response.

The structural model consists of 3 main elements, the wing, leading edge flap and the aileron, as shown in figure 12. These 3 components are modelled using shell elements with the thikness varying from 0.75m at the root to 0.05m at the tip. It is assumed that the control surfaces are locked and hence these components are linked together via solid connections. The material properties were chosen to be those of aluminum. This gave the

American Institute of Aeronautics and Astronautics
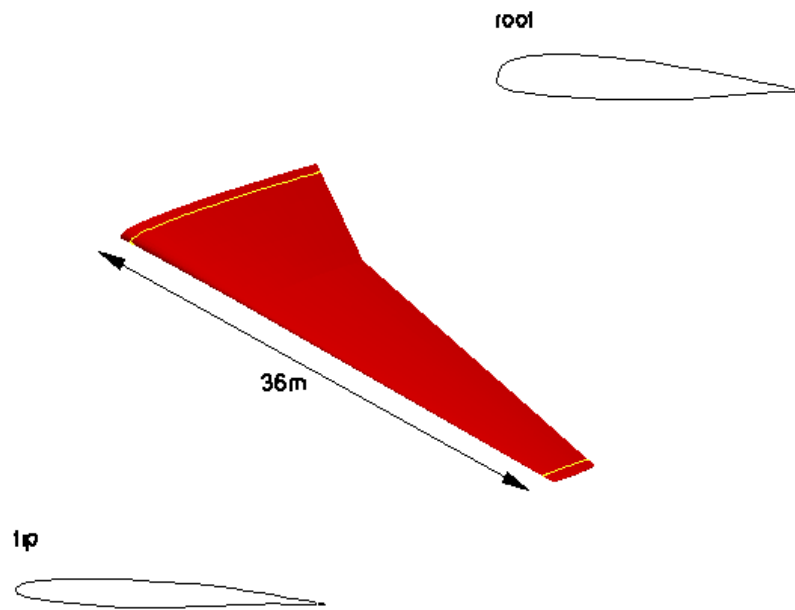
Summary of Geometry
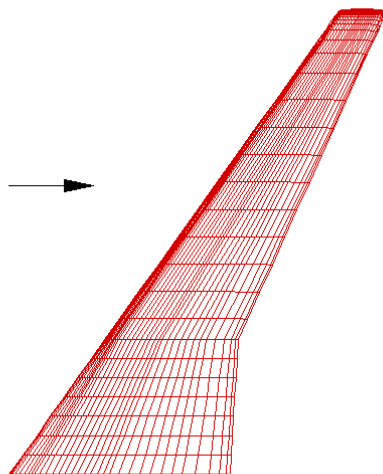
Surface Grid

Figure 8. MDO wing geometry and surface grid.

0.88 Hz
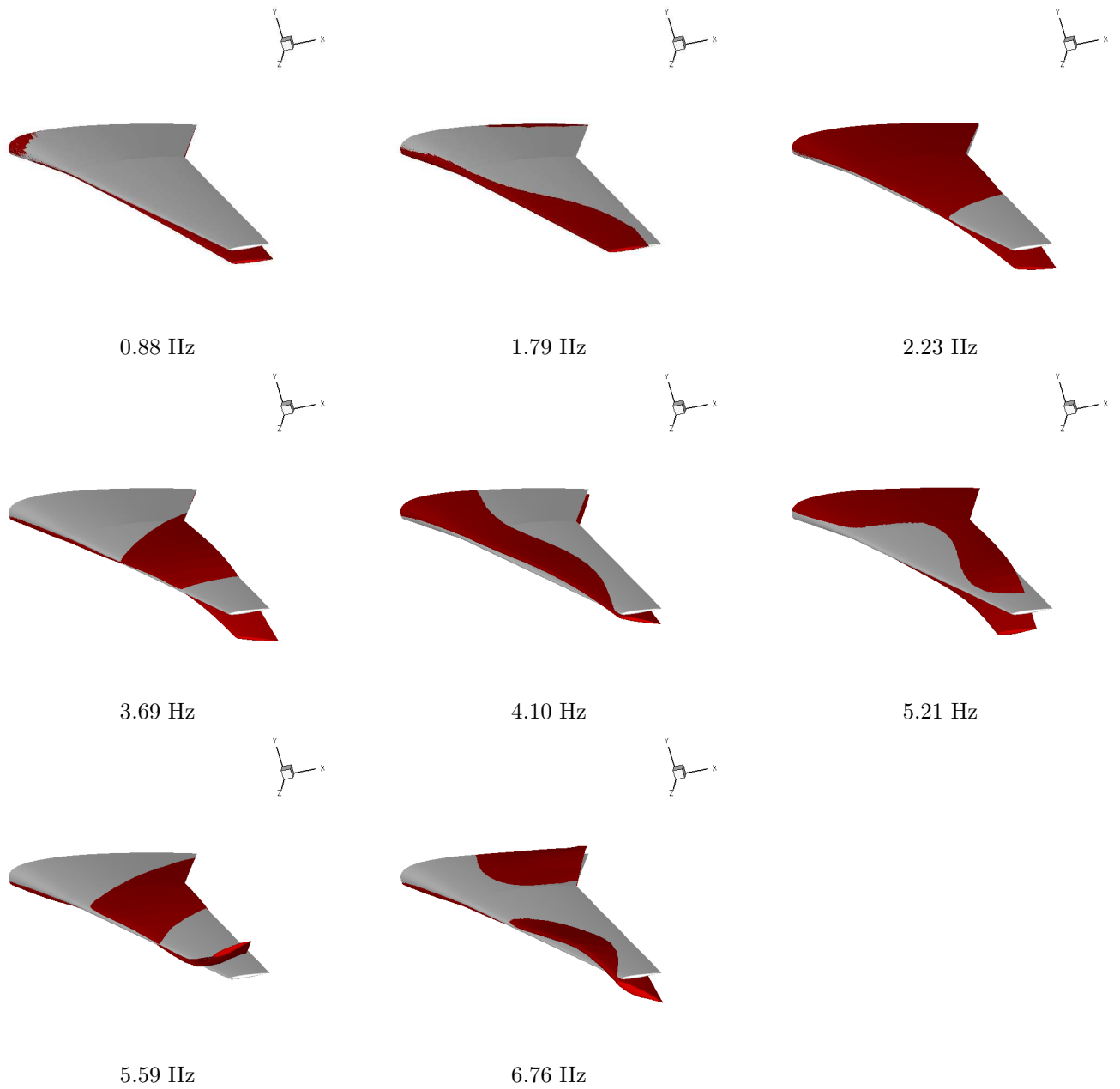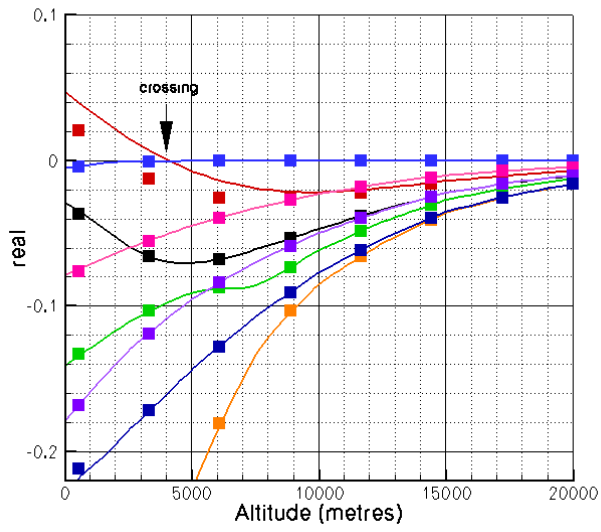
1.79 Hz

2.23 Hz

3.69 Hz

4.10 Hz

5.21 Hz

5.59 Hz

6.76 Hz

Figure 9. Modes shapes defined on the CFD surface grid for the MDO wing.

American Institute of Aeronautics and Astronautics
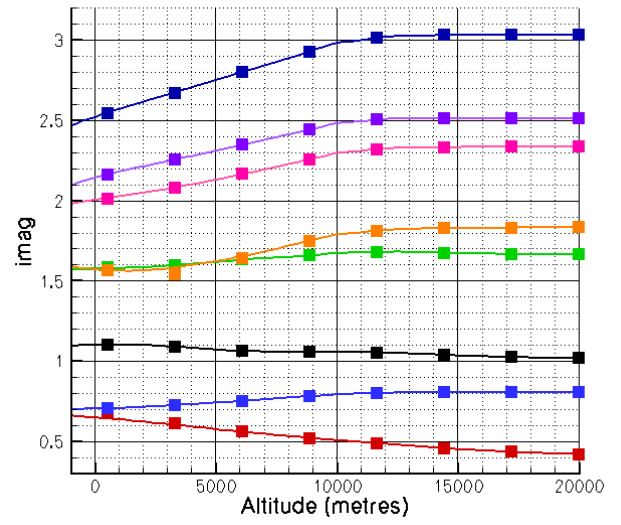
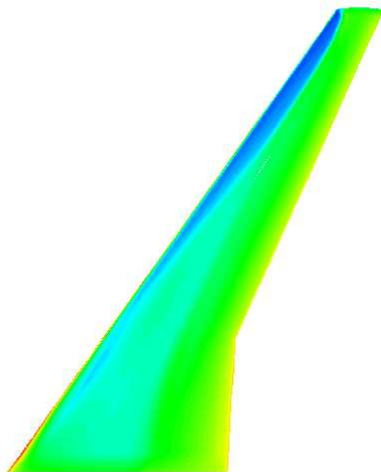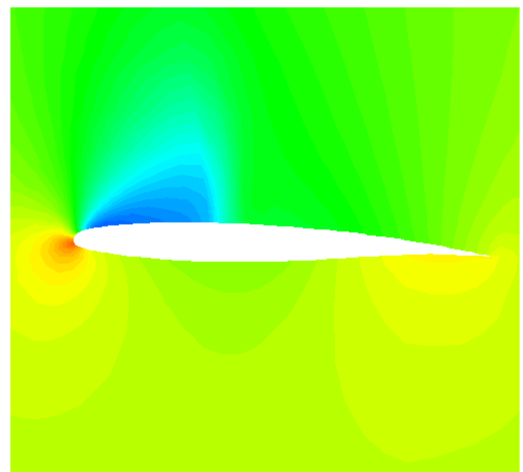real   imaginary

Figure 10. MDO configuration.

upper surface   cut at 80% span

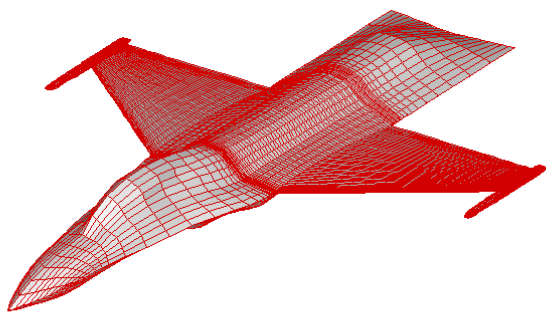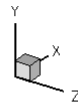**Figure 11. Pressure coefficient distributions for MDO wing.**

American Institute of Aeronautics and Astronautics

first symmetric wing bending mode at 5Hz and the wing torsion at 16Hz, which are close to the values for the **F-16 clean wing** quoted in reference.[19] To obtained a case which flutters around sea level, the wing was then weakened by reducing the Young's modulus by a factor of 2.5.

Calculations were run for Mach numbers between 0.80 and 1.00 in steps of 0.05, and zero degrees angle of attack. The surface pressure distribution is shown in figure 14 and shows a weak shock over the wing. The correction matrices were calculated and the series approach used to trace the eigenvalues for altitudes between -5000 to 15000 metres. The steady state calculation took around 15 minutes on 32 processors, and the generation of the correction matrix for each mode took around 45 minutes.
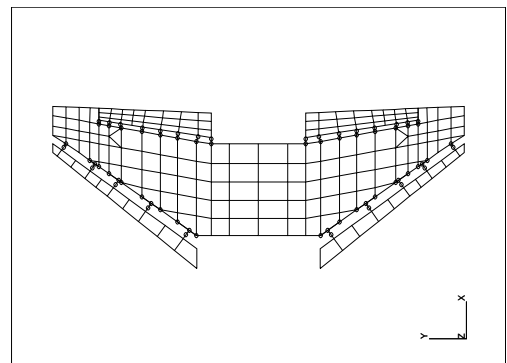
The variation of the real and imaginary parts of the modes is shown for Mach 0.85 in figure 15. The symmetric wing bending mode interacts with the symmetric and asymmetric wing torsion modes to produce flutter at about 3000 metres below seas level.
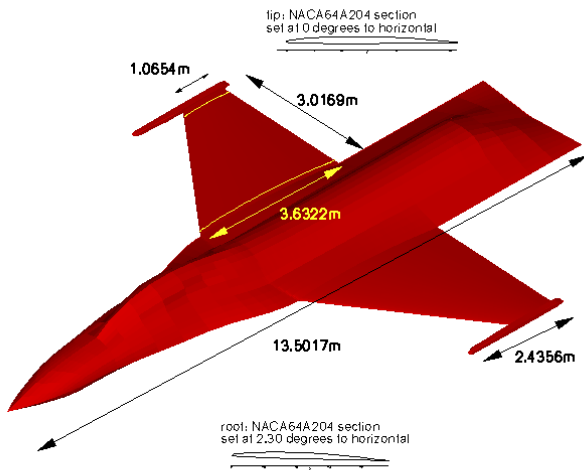
Summary of Geometry

CFD surface grid   FE Grid

Figure 12. Generic fighter geometry and surface CFD and FEM grids.

American Institute of Aeronautics and Astronautics

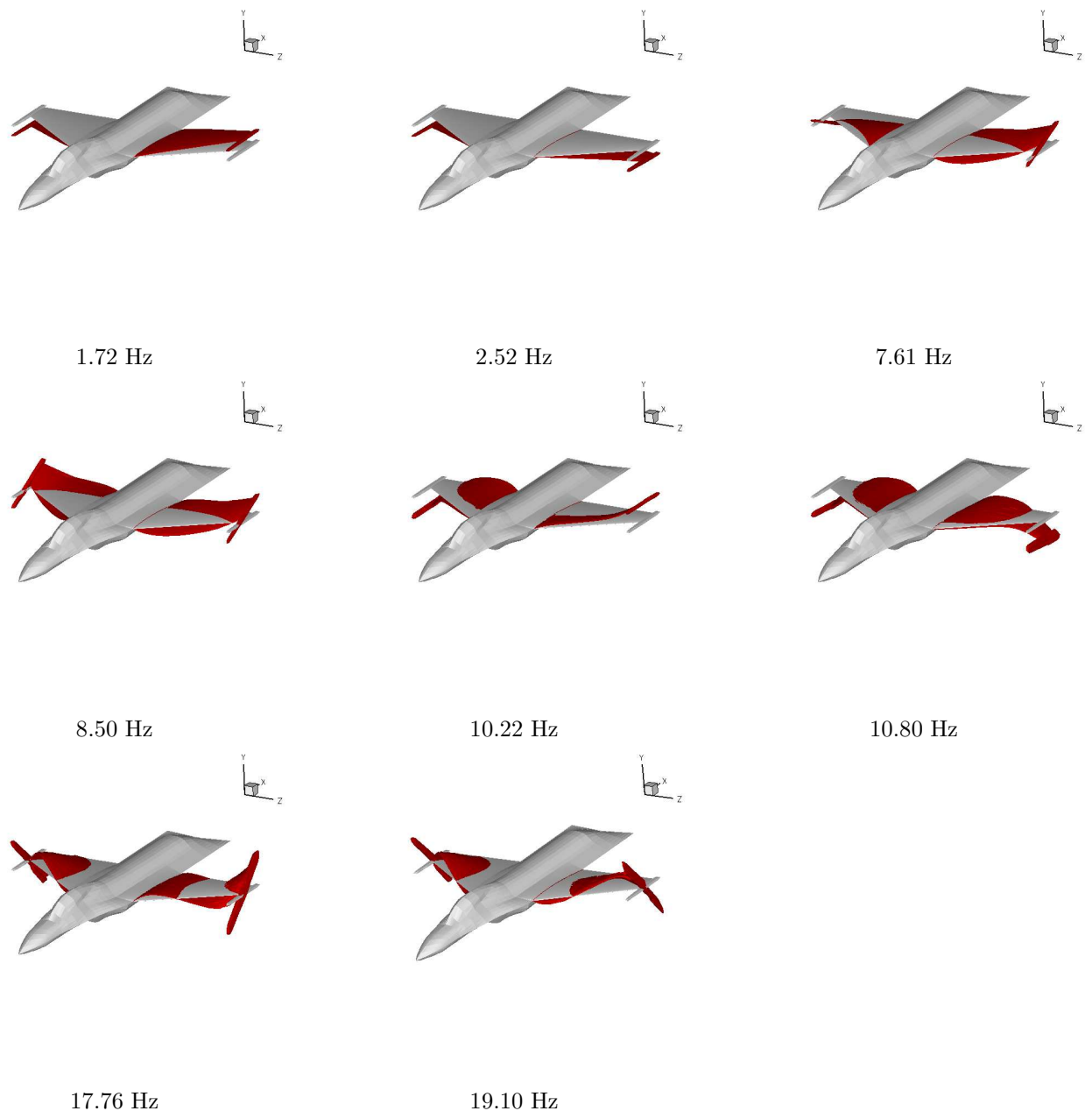| 1.72 Hz | 2.52 Hz | 7.61 Hz |
| 8.50 Hz | 10.22 Hz | 10.80 Hz |
| 17.76 Hz | 19.10 Hz | |

Figure 13. Modes shapes defined on the CFD surface grid for the Generic Fighter.

VII.   Conclusions

A new method for computing aeroelastic stability was proposed and demonstrated. The following conclusions are drawn:

- The use of the Schur complement eigenvalue formulation has allowed large models to be computed by removing the need to solve large sparse linear systems which are almost singular, as in previous work.

- The solution of the small nonlinear Schur eigenvalue problem can be done rapidly, meaning that mode tracking using small parameter steps can be used.

- The series expansion method proved reliable when compared with the nonlinear method.

- Test cases have been computed for the Goland and MDO wings, SST rudder buzz and a generic fighter configuration.

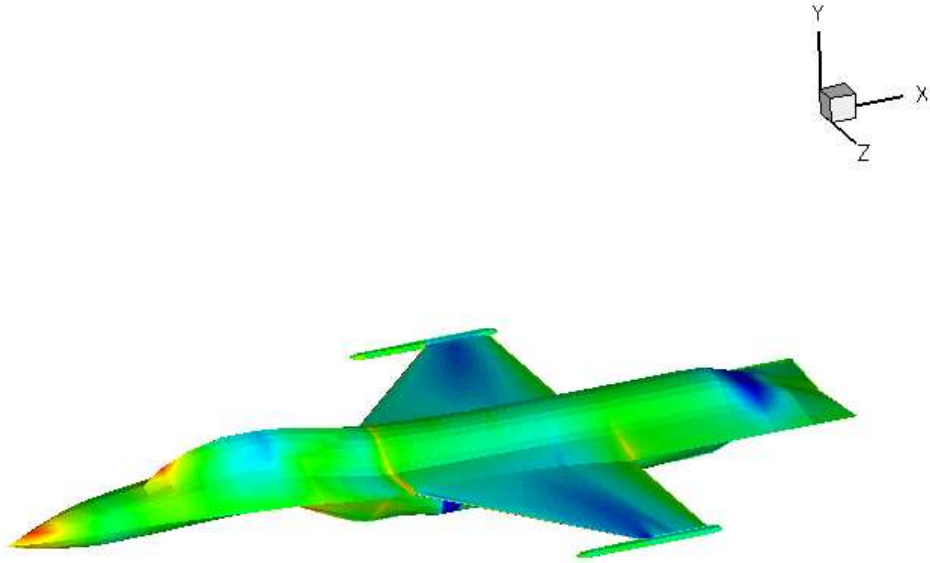American Institute of Aeronautics and Astronautics

Figure 14. Pressure coefficient surface pressure coefficient contours for Generic Fighter at Mach 0.85.

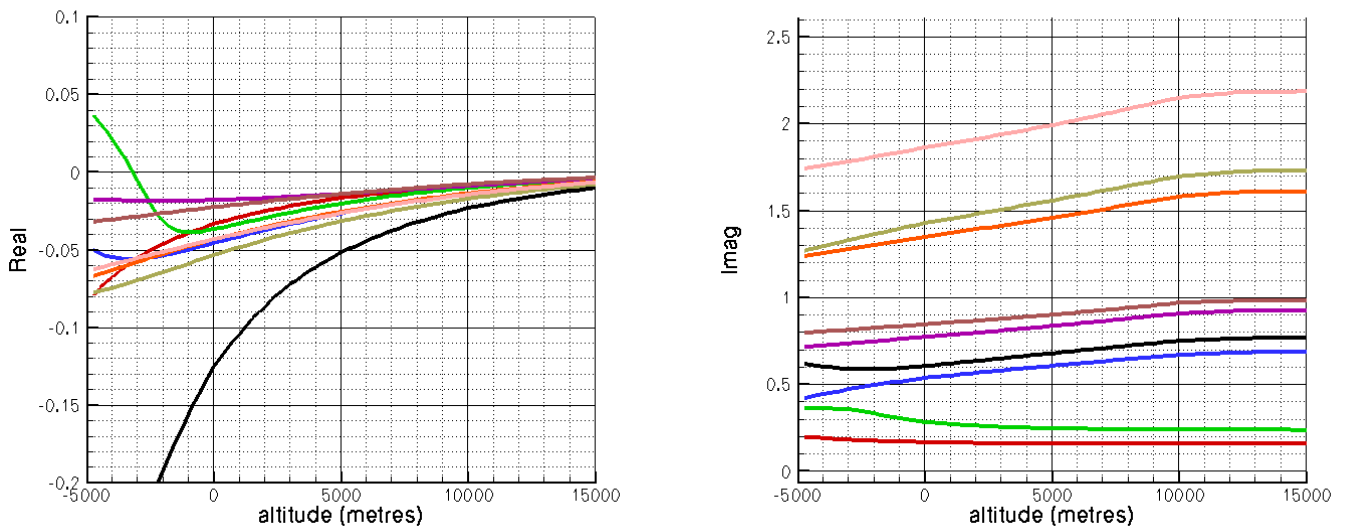Figure 15. Variation of Real and Imaginary parts with altitude for Generic Fighter at Mach 0.85.

American Institute of Aeronautics and Astronautics

- The cost of computing the eigenvalue locii over the range of altitude varies with the square of the number of modes, and is between 5 and 60 times the cost of a steady state solution for the same problem.

- The method provides detailed information about the interaction of normal modes, giving insight into the flutter mechanism.

VIII.   Acknowledgements

References

[1]Woodgate, M.A, Badcock, K.J., Rampurawala, A.M., Richards, B.E., Nardini, D and Henshaw, M.J., Aeroelastic Calculations for the Hawk Aircraft Using the Euler Equations, J Aircraft, 40(4), 2005, 1005-1012.

[2]Lucia, D.J., Beran, P.S. and Silva, W.A, Reduced-order modeling: new approaches for computational physics, Progress in Aerospace Sciences, 40(1-2), 51-117, 2004.

[3]Thomas, J.P., Dowell, E.H., Hall, K.C. and Denegri, C.M., An investigation of the sensitivity of F-16 fighter flutter onset and Limit Cycle Oscillations to Uncertainties, AIAA-2006-1847, 47th AIAA/ASME/ASCE/AHS/ASC Structures. Structural Dynamics and Materials Conference, Newport, Rhode Island, May, 2006.

[4]Morton, S.A. and Beran, P.S., Hopf-Bifurcation Analysis of Airfoil Flutter at Transonic Speeds, Journal of Aircraft, 36, pp 421-429, 1999.

[5]Badcock, K.J., M.A. Woodgate, M.A. and Richards, B.E., The Application of Sparse Matrix Techniques for the CFD based Aeroelastic Bifurcation Analysis of a Symmetric Aerofoil, AIAA Journal, 42(5), 883-892, May, 2004.

[6]Badcock, K.J., Woodgate, M.A. and Richards, B.E., Direct Aeroelastic Bifurcation Analysis of a Symmetric Wing Based on the Euler Equations, Journal of Aircraft, 42(3),731-737, 2005.

[7]Woodgate, M.A. and Badcock, K.J., On the fast prediction of Transonic Aeroelastic Stability and Limit Cycles, AIAA Journal, 45(6), 2007, 1370-1381.

[8]Bekas, K. and Saad, Y., Computation of Smallest Eigenvalues using Spectral Schur Complements, SIAM Journal of Scientific Computing, 27(2), 2005, 458-481.

[9]Badcock, K.J., Woodgate, M.A., Allen, M.R. and Beran, P.S., Wing Rock Limit Cycle Oscillation Prediction Based on Computational Fluid Dynamics, to appear in AIAA Journal, 2008.

[10]Eisenstat, S.C., Elman, H.C. and Schultz, M., Variational Iterative Methods for Nonsymmetric Systems of Linear Equations, SIAM Journal of Numerical Analysis, Vol. 20, No. 2, April 1983, 345-357.

[11]Saad, Y and Sosonkina, M, pARMS : A package for the parallel iterative solution of general large sparse linear systems user's guide. Report UMSI2004-8, Minnesota Supercomputer Institute, University of Minnesota, Minneapolis, MN, 2004.

[12]Beran, P.S., Knot, N.S., Eastep, F.E., Synder, R.D. and Zweber, J.V., Numerical Analysis of Store-Induced Limit Cycle Oscillarion, Journal of Aircraft, 41(6), 1315-1326, 2004.

[13]Matsushita, H., Tamayama, M., Saitoh, K. and Nakamichi, J, NAL SST arrow wing with oscillating flap. In *Verification an Validation Data for Computational Unsteady Aerodynamics*, pages 295–318. RTO Technical Report–26, October 2000.

[14]Rampurawala, A.M. and Badcock. K.J., Evaluation of a Simplified Grid Treatment for Oscillating Trailing-Edge Control Surfaces, Journal of Aircraft, 44(4), 1177-1188, 2007.

[15]Rampurawala. A.M., Aeroelastic Analysis of Aircraft with Control Surfaces using CFD, PhD Thesis, University of Glasgow, Glasgow, U.K., 2006.

[16]Girodroux-Lavigne, P., Grisval, J. P., Guillemot, S., Henshaw, M., Karlsson, A., Selmin, V., Smith, J., Teupootahiti, E. and Winzell, B., Comparison of static and dynamic fluid-structure interaction solutions in the case of a highly flexible modern transport aircraft wing, Aerospace Science and Technology, 7, 2003, 121-133.

[17]Allen, C.B., Jones, D., Taylor, N.V., Badcock, K.J., Woodgate, M.A., Rampurawala, A.M., Cooper, J.E. and Vio, G.A., A Comparison of Linear and Nonlinear Flutter Prediction Methods: A Summary of PUMA DARP Aeroelastic Results, Aeronautical Journal, 110 (1107), May, 2006, 333-343.

[18]Goura, G.S.L., Badcock, K.J. and Woodgate, M.A., Extrapolation Effects on Coupled Computational Fluid Dynamics/Computational Structural Dynamics Simulations, AIAA Journal, 41(2), February, 2003, 312-314.

[19]Cattarius, J, Numerical Wing/Store Interaction Analysis of a Parametric F-16 Wing,PhD Thesis, Virginia Polytechnic Institute and State University, Blacksburg, Virginia, U.S., 1999.